Intraoperative localization of lymph node metastases with a replication-competent herpes simplex virus

Prasad S. Adusumilli, MD,[a] David P. Eisenberg, MD,[a] Brendon M. Stiles, MD,[a] Sun Chung, MD,[b] Mei-Ki Chan, BS,[a] Valerie W. Rusch, MD,[a] and Yuman Fong, MD[a]

Supplemental material is available online.

From the Departments of Surgery[a] and Pathology,[b] Memorial Sloan-Kettering Cancer Center, New York, NY.

Supported in part by AACR-Astra Zeneca Cancer Research and Prevention Foundation Fellowship (P.S.A), grants RO1 CA 75416 and RO1 CA/DK80982 (Y.F.) from the National Institutes of Health, grant MBC-99366 (Y.F.) from the American Cancer Society, grant BC024118 from the US Army (Y.F.), grant IMG0402501 from the Susan G. Komen Breast Cancer Foundation (Y.F. and P.S.A.), and grant 032047 from Flight Attendant Medical Research Institute (Y.F. and P.S.A.) and Mr William H. Goodwin and Mrs Alice Goodwin and the Commonwealth Foundation for Cancer Research grant–The Experimental Therapeutics Center of Memorial Sloan-Kettering Cancer Center (Y.F.).

Read at the Eighty-sixth Annual Meeting of The American Association for Thoracic Surgery, Philadelphia, Pa, April 29-May 3, 2006.

Received for publication April 6, 2006; revisions received July 7, 2006; accepted for publication July 12, 2006.

Address for reprints: Yuman Fong, MD, Department of Surgery, Memorial Sloan-Kettering Cancer Center, 1275 York Ave, New York, New York 10021 (E-mail: fongy@mskcc.org).

J Thorac Cardiovasc Surg 2006;132:1179-88

0022-5223/$32.00

doi:10.1016/j.jtcvs.2006.07.005

Objectives: Lymph node status is the most important prognostic factor determining recurrence and survival in patients with mesothelioma and other thoracic malignancies. Accurate localization of lymph node metastases is therefore necessary to improve selection of resectable and curable patients for surgical intervention. This study investigates the potential to identify lymph node metastases intraoperatively by using herpes-guided cancer cell–specific expression of green fluorescent protein.

Methods: After infection with NV1066, a herpes simplex virus carrying green fluorescent protein transgene, human mesothelioma cancer cell lines were assessed for cancer cell–specific infection, green fluorescent protein expression, viral replication, and cytotoxicity. Murine models of lymphatic metastasis were established by means of surgical implantation of cancer cells into the preauricular (drainage to cervical lymph nodes) and pleural (mediastinal and retroperitoneal lymph nodes) spaces of athymic mice. Fluorescent thoracoscopy, laparoscopy, and stereomicroscopy were used to localize lymph node metastases that were confirmed by means of immunohistochemistry.

Results: In vitro NV1066 infected, replicated (5- to 17,000-fold), and expressed green fluorescent protein in all cancer cells, even when infected at a low ratio of one viral plaque-forming unit per 100 tumor cells. In vivo NV1066 injected into primary tumors was able to locate and infect lymph node metastases producing green fluorescent protein that was visualized by means of fluorescent imaging. Histology confirmed lymphatic metastases, and immunohistochemistry confirmed viral presence in regions that expressed green fluorescent protein.

Conclusions: Herpes virus–guided cancer cell–specific production of green fluorescent protein can facilitate accurate localization of lymph node metastases. Fluorescent filters that detect green fluorescent protein can be incorporated into operative scopes to precisely localize and biopsy lymph node metastases.

Malignant pleural mesothelioma (MPM) is an aggressive cancer with a median survival of 4 to 12 months in untreated patients.[E1] In patients with early-stage disease treated by means of surgical resection, a 5-year survival rate of 46% has been reported in patients who undergo extrapleural pneumonectomy and have the favorable features of epithelial histology and the absence of mediastinal lymph node (LN) involvement.[E2] However, approximately

Abbreviations and Acronyms

CT = computed tomography
GFP = green fluorescent protein
HSV = herpes simplex virus
LN = lymph node
MOI = multiplicity of infection
MPM = malignant pleural mesothelioma
PBS = phosphate-buffered saline
PET = positron emission tomography
RT-PCR = reverse transcriptase–polymerase chain reaction

20% to 30% of patients undergo exploratory thoracotomy without resection because of the unreliability of computed tomographic (CT) and magnetic resonance imaging scans in predicting mediastinal nodal metastases and locally advanced disease.[E3,E4] Nodal size measured on a CT scan is not sensitive to determine the presence or absence of metastases.[E3] Recent studies have shown that even positron emission tomographic (PET) scans failed to reliably identify the mediastinal nodal metastases.[E5] Pleural tumor involving or abutting the mediastinum might show increased fluorodeoxyglucose (FDG) uptake and can be misinterpreted as nodal disease.[E5] Therefore any management decision based on PET findings of N2 disease requires confirmation by means of surgical pathologic evaluation because of the known adverse effect of N2 disease on prognosis.[E5] Accurate localization of LN metastases is therefore necessary to improve selection of resectable and curable patients for surgical intervention.[E6] Cervical mediastinoscopy, thoracoscopy, and laparoscopy have emerged as valuable diagnostic procedures for patients with MPM who are considered candidates for surgical-based therapy.[E3,E7,E8] The development of a real-time in vivo technique that might enhance accurate detection of metastatic LNs is essential to further increase the sensitivity and specificity of mediastinoscopy and other endoscopic methods.

Herpes simplex virus (HSV) type 1–mediated oncolysis has emerged as a novel treatment modality against MPM.[E9-E14] Studies published from our laboratory and others have shown that these viruses are safe and effective in reducing the tumor burden both in animal models[E9-E12] and in human subjects.[E14] Oncolysis results from the replicative lifecycle of the virus, which lyses infected tumor cells and releases viral progeny for further infection and killing of neighboring cancer cells.[E15-E17] NV1066 is one such genetically engineered, multimutated, replication-competent, oncolytic HSV-1 virus.[E18] We have demonstrated the efficacy of NV1066[E9,E11] and other oncolytic HSV viruses, G207 and NV1020, in the treatment of MPM both in vitro and in vivo. NV1066 has deletions of one copy of each of the genes *ICP0*, $\gamma_1 34.5$, and *ICP4* to attenuate the virus from natural toxicities and help ensure that it preferentially replicates within cancer cells.[E18] Genetically engineered herpes viruses might be useful in cancer therapy based on their oncolytic properties alone[E9,E19] or as vectors to carry therapeutic,[E20] immunomodulatory,[E21] or imaging transgenes[E10,E22,E23] to targeted tumors. NV1066 carries such a marker gene, a constitutively expressed transgene for enhanced green fluorescent protein (GFP) that is identifiable 2 to 4 hours after viral entry into cells.[E10,E22,E23] In the current study we hypothesized that the tumor specificity of NV1066 can be exploited for detection of metastases in LNs. In our animal models of MPM, we have demonstrated that the treatment of primary tumors results in the infection and GFP expression of metastatic tumor in LNs and aids in their detection.

Materials and Methods

Cell Culture

The human malignant mesothelioma cell lines VAMT, H-28, H-2052, H-2373 (sarcomatoid), H-2452, H-meso (epithelioid), H-meso1A, MSTO-211H, JMN (biphasic), Meso-9, and Meso-10 were studied. MSTO-211H cells, H28 mesothelioma cells, and Vero cells (from the African green monkey kidney) were obtained from the American Type Culture Collection (ATCC, Rockville, Md). H-meso and H-meso1A cell lines were obtained from the National Cancer Institute (NCI, Bethesda, Md). JMN, VAMT, Meso-9, and Meso-10 cell lines were a kind donation from Dr Sirotnik from Memorial Sloan-Kettering Cancer Center (New York, NY). H-2052, H-2452, and H-2373 cell lines were a kind donation from Dr Pass from Karmanos Cancer Institute, Wayne State University (Detroit, Mich). All the cell lines were grown in appropriate media and were incubated in a humidified incubator supplied with 5% CO_2.

Virus

NV1066 is a replication-competent, attenuated HSV-1 oncolytic virus that has been described previously.[E18] A single copy of the *ICP4*, *ICP0*, and $\gamma_1 34.5$ genes was deleted in NV1066 to decrease viral virulence and increase tumor specificity. An enhanced GFP sequence under the control of a constitutive cytomegalovirus promoter is inserted into the viral backbone. Because of this insertion, NV1066-infected cancer cells express green fluorescence when observed by means of fluorescent imaging methods.[E23] All virus preparations were formulated in D–phosphate-buffered saline (PBS) solution−10% glycerin and stored at −80°C. Viral stocks were propagated on Vero cells, harvested by means of freeze-thaw lysis and sonication, and titered by using a standard plaque assay.

Vector Spread Assay

Vector propagation, as analyzed by GFP expression, was determined by means of FACS analysis at a viral infective dose of a multiplicity of infection (MOI; ie, ratio of viral plaque-forming units to tumor cell) of 0.01, 0.1, or 1. The percentage of GFP-positive cells compared with control cells without viral infection was analyzed on each day to day 7. Cells were harvested with 0.25% trypsin in 0.02% ethylenediamine tetra-acetic acid, centri-

fuged, washed in PBS, and brought up in 100 μL of PBS. Five microliters of 7-amino-actinomycin (BD Pharmingen, San Diego, Calif) was added as an exclusion dye for cell viability. Data for GFP expression was acquired on a FACS Calibur machine equipped with Cell Quest software (Becton Dickinson, San Jose, Calif). All samples were performed in triplicate.

Viral Replication Assay

The ability of the oncolytic virus to replicate within MPM cells was evaluated by using a viral plaque assay, as described previously.[E9] All samples were performed in triplicate.

Cytotoxicity Assay

NV1066 cytotoxicity on MPM cells was determined on each day for 7 days by means of a standard lactate dehydrogenase release bioassay. All samples were tested in 6 wells. Experiments were repeated at least 3 times to ensure reproducibility.

Cancer Cell–specific GFP Expression

NV1066-induced GFP expression in cancer cells was assessed by means of fluorescent microscopy. Cancer cells (5×10^4 in 500 μL of media) were incubated in 4-well chamber slides (Lab-Tek, San Diego, Calif) and were infected with NV1066 at MOIs of 0.01, 0.1, or 1.0 in 100 μL of PBS. Cells treated with PBS alone served as control cells. In additional wells, cancer cells were coincubated with lymphocytes isolated from normal murine LNs. Before imaging, cells were stained with 1 μg/mL of the double-stranded, DNA-specific fluorochrome Hoechst 33342 (NPE Systems, Inc, Pembroke Pines, Fla). Slides were then examined with a Zeiss Axiovert 200M inverted stand microscope (Carl Zeiss, Inc, Oberkochen, Germany) and the MetaMorph Imaging System (Universal Imaging Corp, Downingtown, Pa). Identical microscopic fields were examined with a bright-field, DAPI fluorescent filter to detect Hoechst nuclear staining and with a fluorescent filter fixed at 470 ± 40 nm to detect GFP expression.

Animal Experiments

Animal experiments were performed with the approval of the Memorial Sloan-Kettering Institutional Animal Care and Use Committee. Six- to 8-week-old male athymic mice (National Cancer Institute) were housed in temperature- and light-controlled rooms. Food and water were provided ad libitum. Mice were anesthetized with inhalational isoflurane for all procedures and killed by means of CO_2 inhalation at the termination of the experiment.

Lymphatic Metastasis Animal Models

One percent isosulfan blue dye (50 μL) was injected into the preauricular or pleural spaces of mice (n = 3) to confirm the normal lymphatic drainage pattern in mice. Minutes after the injection, the animals were killed, and the bilateral cervical, mediastinal, and retroperitoneal LN basins were surgically exposed. Draining LNs were identified by the presence of uptake of blue dye (data not shown). Lymphatic metastasis animal models were developed by means of injection of 5×10^6 cancer cells in 50 μL of PBS into the preauricular (n = 20) or intrapleural (n = 20) spaces of athymic male nude mice. Tumors were then permitted to grow for 4 to 8 weeks to allow for the development of LN metastases. Cervical, mediastinal, and retroperitoneal LN basins were examined after killing the animals.

Localization of LN Metastases

Four to 8 weeks after tumor implantation (n = 20), animals were treated with 5×10^6 plaque-forming units of NV1066 in 50 μL of PBS (intratumoral or intrapleural) on treatment days 0 and 7. Forty-eight hours after the second treatment, mice were killed, and the LN basins were surgically exposed. These areas were then imaged with the Leica MZFL3 Stereomicroscope (Leica Microsystems, Wetzlar, Germany) in both bright-field and fluorescent modes. GFP expression is detected by using an excitation filter fixed at 470 nm to accommodate the excitation peak of 475 nm and an emission filter fixed at 500 nm to accommodate the emission peak of 509 nm. The Retiga EX digital CCD camera (Qimaging, Burnaby, BC, Canada) was used for image capture.

Fluorescent Thoracoscopy

We used an endoscopic system developed in collaboration with Olympus America, Inc (Scientific Equipment Division, Melville, NY), which images in both bright-field and fluorescent modes, permitting the detection of GFP. The mechanics of this endoscope have been described previously.[E24] A control button incorporated directly into the camera head enables rapid exchange between bright-field and fluorescent modes. GFP images were taken with minimal background illumination to illustrate the surrounding organs. By using this system, each mouse (n = 6) was systematically examined for the presence of metastatic LNs, as determined by the presence of green fluorescence. Animals with disease treated with PBS (n = 3) and animals without disease treated with NV1066 (n = 3) were used as negative control animals.

Viral Specificity for Tumor

Immediately after tissue imaging, LNs (both green and not green) were harvested, embedded in Tissue-Tek O.C.T compound (Sakura Finetek, Torrance, Calif), and frozen in liquid nitrogen. Representative samples were also fixed in 10% buffered formalin acetate and embedded in paraffin. The nodes (n = 100) were sectioned (8-μM sections) for histologic examination. After fixation, slides were first examined under fluorescent microscopy for GFP expression and then stained with hematoxylin and eosin to determine whether GFP expression localized to the foci of cancer. Alternate sections that expressed GFP were stained with rabbit polyclonal HSV-1 antibody by using a Histomouse-SP Bulk Staining Kit (Zymed Laboratories Inc, San Francisco, Calif) to confirm that GFP expression in LNs is indeed due to viral infection. Four representative fields for each microscopic section were examined. An institutional animal pathologist confirmed all results.

Statistical Analysis

All data were expressed as means ± standard error of the mean. Comparisons between groups were made by using the 2-tailed Student *t* test.

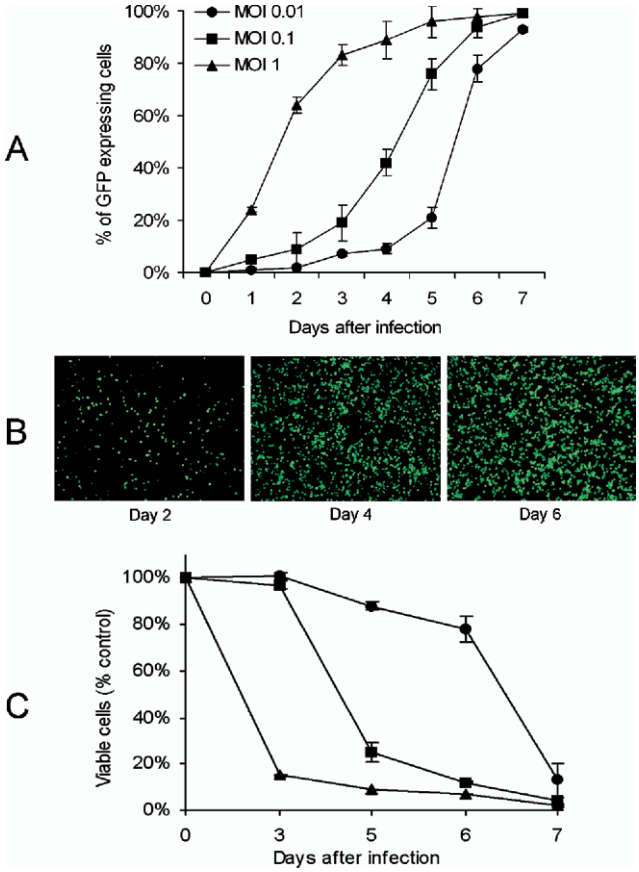

Figure 1. NV1066 infects, expresses green fluorescent protein *(GFP)* in, propagates in, and lyses malignant mesothelioma cells. NV1066-infected MSTO-211H mesothelioma cells express GFP, as determined by means of flow cytometry (A) and fluorescent microscopy (B). GFP-expressing cells increased over time, to nearly 100% at all multiplicities of infection (*MOIs*; A). Even when infected at a low MOI of 0.1 (B), over time, NV1066 replicates within and propagates among mesothelioma cells, as evident by an increasing percentage of GFP-positive cells observed under fluorescent microscopy. NV1066 effectively kills MSTO-211H cells at all MOIs of 0.01 *(circles)*, 0.1 *(squares)*, or 1 *(triangles)*, as assessed by means of the lactate dehydrogenase colorimetric cytotoxicity assay. Results were expressed as percentages of live cells compared with control untreated cells grown under identical conditions.

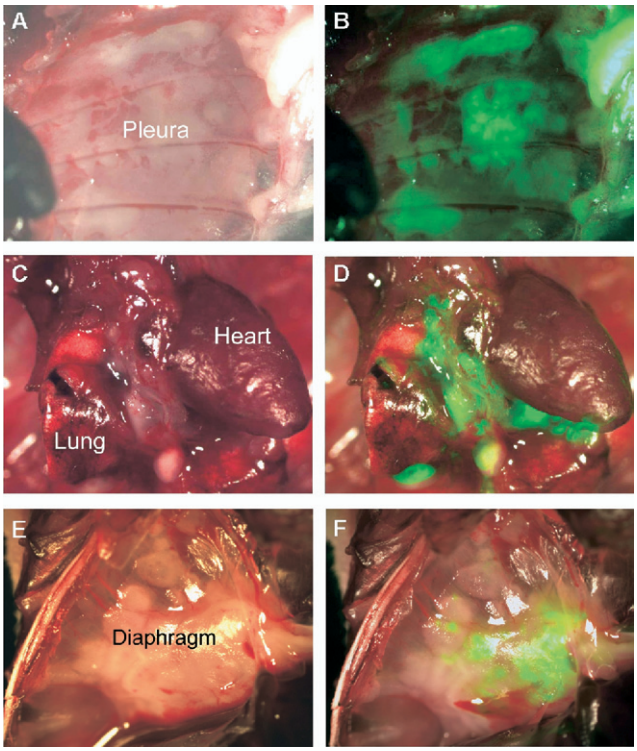

Figure 2. NV1066 selectively infects pleural, mediastinal, and diaphragmatic mesothelioma and spares normal tissue. After intrapleural administration of a single dose of NV1066, the pleural cavities of mice with macroscopic malignant mesothelioma were examined in bright-light (A, C, and E) and green fluorescent protein (*GFP*; B, D, and F) modes by using fluorescent microscopic systems. GFP expression was localized to pleural (B), mediastinal (D), and diaphragmatic (F) mesothelioma, sparing normal tissues.

Results

NV1066 Infects, Expresses GFP in, Replicates in, and Lyses Malignant Mesothelioma Cells

In vitro NV1066 effectively infected and expressed GFP in MPM cells (MSTO-211H) at all MOIs of 0.01, 0.1, and 1. NV1066-infected cells expressed GFP, as measured by means of flow cytometry (Figure 1, *A*) and fluorescent microscopy (Figure 1, *B*). After treatment with NV1066 at MOIs of 0.01, 0.1, and 1.0 in MSTO-211H cells, 79%, 94%, and 98% of the cells, respectively, expressed GFP by day 6 (Figure 1, *A*; $P < .001$ vs untreated control cells), as measured by means of flow cytometry. NV1066 was able to replicate efficiently in MPM cells. After infection at MOIs of 0.01, 0.1, and 1.0, NV1066 is able to replicate more than 17,000-fold, 1400-fold, and 64-fold compared with the initial infecting dose. After in vitro treatment with NV1066, higher peak viral titers often occur after lower initial MOIs because early cell death in the populations that are treated with the higher MOIs limits the cell number for productive cellular replication of virus. With progressive viral replication and vector spread, the percentage of GFP-expressing cells increased over time (Figure 1, *B*). Furthermore, NV1066 demonstrates dose- and time-dependent cytotoxicity over a 100-fold range of viral doses (Figure 1, *C*). Three days after infection at an MOI of 1.0, 85% ± 2% of cells were killed. By day 7, nearly 100% of cells were killed. Seven days after infection at a 10-fold lower MOI (0.1), 96% ± 4% of cells were killed. Even at an MOI of 0.01,

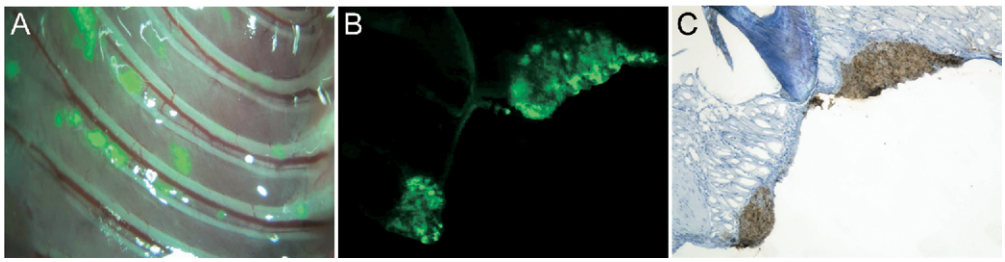

Figure 3. NV1066-induced green fluorescent protein (*GFP*) expression facilitates accurate tumor localization. NV1066-induced tumor-specific GFP expression facilitated selective biopsy of pleural nodules by means of thoracoscopy (A). Serial sectioning was performed and examined with a fluorescent microscope, confirming GFP expression to the cancer nodules (B). Corresponding cut sections were stained with polyclonal herpes simplex virus (*HSV-1*) antibody (C). Viral infection was localized to the cancer nodules. No GFP expression or viral staining was evident in normal tissue.

representing 1 viral particle per 100 cancer cells, 87% ± 4% of cells are killed 7 days after infection. The increase in cells killed observed at 4 to 6 days at lower MOIs of 0.01 and 0.1, coinciding with increasing viral titers, indicates that NV1066 was able to successfully replicate within and propagate among MPM cells. Similar results were reproduced in other MPM cells.

NV1066 Selectively Infects and Expresses GFP in Mesothelioma

After intrapleural administration of NV1066, GFP expression was visualized easily by means of fluorescent microscopy in pleural tumor models. A single dose of virus was able to replicate in, spread, and infect pleural (Figure 2, *A* and *B*), mediastinal (Figure 2, *C* and *D*), and diaphragmatic (Figure 2, *E* and *F*) mesothelioma, sparing normal tissue. These representative figures demonstrate the tumor-specific infectious ability of NV1066 in a pleural mesothelioma model. Cancer cell−specific GFP expression was evident by means of fluorescent thoracoscopy in other mice treated with NV1066 and is absent in mice treated with PBS.

GFP Expression Can Facilitate Accurate Tumor Localization and Biopsy

After the intrapleural administration of NV1066, within 48 hours fluorescent thoracoscopy (Figure 3, *A*) demonstrated strong GFP expression, specifically in tumor nodules (Figure 3, *B*). All sections that expressed GFP were found to have tumor cell infiltrations that correspond to the areas of expression. When a cross-section was taken from the frozen tissue and stained with HSV-1−specific polyclonal antibody, NV1066 infection (Figure 3, *C*) and GFP expression (Figure 3, *B*) were localized clearly to the cancer nodule, and no evidence of infection was noted in normal tissue. Multiple sections studied from different animals confirmed similar results.

NV1066 Selectively Infects Malignant Mesothelioma Cells and Spares Lymphocytes

All MPM cells tested express GFP 2 to 12 hours after viral infection at all MOIs tested. The intensity of GFP expression is several logs higher than background autofluores-

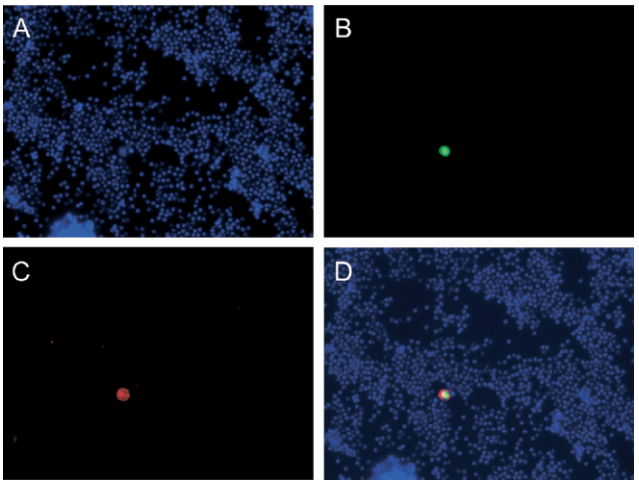

Figure 4. NV1066 selectively infects cancer cells and spares lymphocytes. NV1066 selective infection of cancer cells among a mixture of lymphocytes is confirmed by counterstaining with immunohistochemistry. Human mesothelioma cancer cells were mixed with lymphocytes harvested from normal lymph nodes (*LNs*; A) and incubated with NV1066 for 18 hours. Live cells were identified by means of nuclear Hoechst staining (blue). Examination under a fluorescence microscope identified cancer cells on the basis of expression of strong green fluorescence (B). These mesothelioma cells express integrin (*CD51/61*) surface antigen. Incubation with R-phycoerythrin–conjugated mouse anti-human CD51/61 monoclonal antibody confirmed that green fluorescent protein (*GFP*) expression is selective to only cancer cells (identified by red fluorescence; C). Overlap of fluorescent pictures with a bright field identifies cancer cells among normal cells (D).

GTS

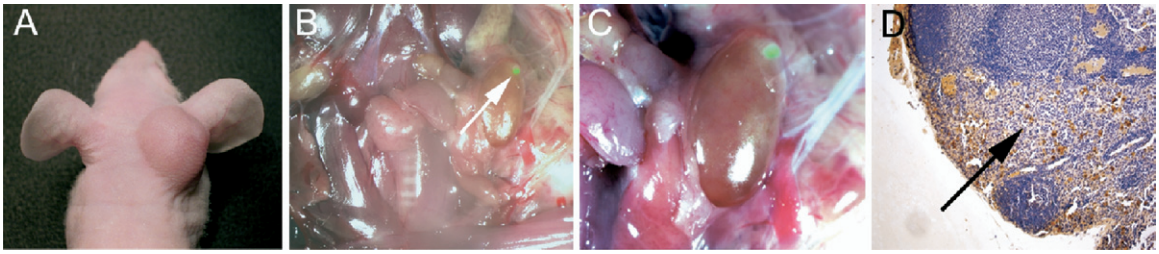

Figure 5. NV1066 treatment of the primary tumor facilitates the selective infection and green fluorescent protein (*GFP*) expression of the metastatic tumor in the lymph nodes (*LNs*). Mesothelioma cells were injected into the preauricular areas of the mice (A). Four to 8 weeks after tumor implantation, primary tumor is treated with NV1066. Mice were killed, and the cervical area was examined under stereomicroscopy for GFP expression (B). The GFP-expressing area of the LN is shown by an *arrow* (B and C). Immunohistochemical staining of the GFP-expressing lymph nodes (LNs) with polyclonal HSV-1 antibody identifies the viral specificity to metastatic sites in LN-sparing germinal centers (D).

cence and can be clearly delineated. We further investigated the ability of NV1066 to induce cancer cell−specific GFP expression in a mixture of cells (n = 6). Normal lymphocytes coincubated with cancer cells, and NV1066 did not express GFP (control cells). Representative figures are shown in Figure 4. Hoechst nuclear staining demonstrates all live cells in the incubated chamber in Figure 4, *A*. Cancer cell−specific GFP expression is seen in Figure 4, *B*. These mesothelioma cells express integrin (CD51/61) surface antigen. Incubation with R-phycoerythrin−conjugated mouse anti-human CD51/61 monoclonal antibody identified mesothelioma cells by means of red fluorescence (Figure 4, *C*). Overlap of fluorescent pictures confirmed that NV1066-induced GFP expression is isolated to cancer cells among normal lymphocytes (Figure 4, *D*). These experiments were repeated in triplicate to ensure reproducibility.

Treatment of the Primary Tumor Aids in Detection of LN Metastases

In a preauricular mouse model of MPM (Figure 5, *A*), after intratumoral injection of NV1066, the cervical area was explored and examined under bright-field and fluorescent modes. Overlap of both modes demonstrates the GFP expression in NV1066-infected tumor metastases in the LNs (Figure 5, *B*). The metastatic area of the LNs exhibited intense focal expression of GFP when imaged with fluorescent stereomicroscopy (Figure 5, *C*). LNs not harboring tumor and control LNs did not express GFP. Immunohistochemistry confirmed viral presence (Figure 5, *D*) in metastatic LNs. Although preauricular tumors were established bilaterally, tumor growth and cervical LN presence differed from animal to animal. Among the cervical LNs, metastatic LNs were clearly identified by means of GFP expression.

GFP Expression Facilitates Minimally Invasive Detection of LN Metastases

Administration of NV1066 into the primary tumor (n = 40) aided identification of LN metastases in both the regional stations and in distant nodes. In a model of intrapleural MPM (n = 20), intrathoracic administration of NV1066 led to selective infection and fluorescence of otherwise inconspicuous nodal metastases in the para-aortic region (Figure 6, *A* and *B*), as well as mediastinal (Figure 6, *C* and *D*) and retroperitoneal (Figure 6, *E* and *F*) LN metastases. LNs that are less than 2 mm in size, smooth in appearance, and histologically deemed negative on a single cut section from a frozen section are considered inconspicuous for this purpose.

NV1066 Selective Infection of Tumor in LNs Is Confirmed by Histology and Immunohistochemistry

Histologic examination confirmed the presence of tumor (Figure 7, *C*; metastatic LN) and GFP (Figure 7, *D*; metastatic LN) in positive LNs, as identified by means of fluorescent stereomicroscopy and thoracoscopy (Figure 7). Furthermore, areas of GFP expression localized to tumor foci in LNs. Absence of tumor and GFP in negative nonfluorescent LNs (as determined by using fluorescent imaging) was similarly confirmed by means of microscopic analysis (Figure 7, *C* and *D*; normal LN). In histologic sections expressing GFP, viral presence in metastatic LNs was confirmed by using HSV immunohistochemistry (Figure 7, *E*; metastatic LN).

Discussion

MPM is a diffuse disease arising in the parietal and diaphragmatic pleura. The natural spread of mesothelioma is to the lungs through the visceral pleura and by local extension into the chest wall and diaphragm. Pleural lymphatics drain into the internal thoracic, peridiaphragmatic, and extrapleu-

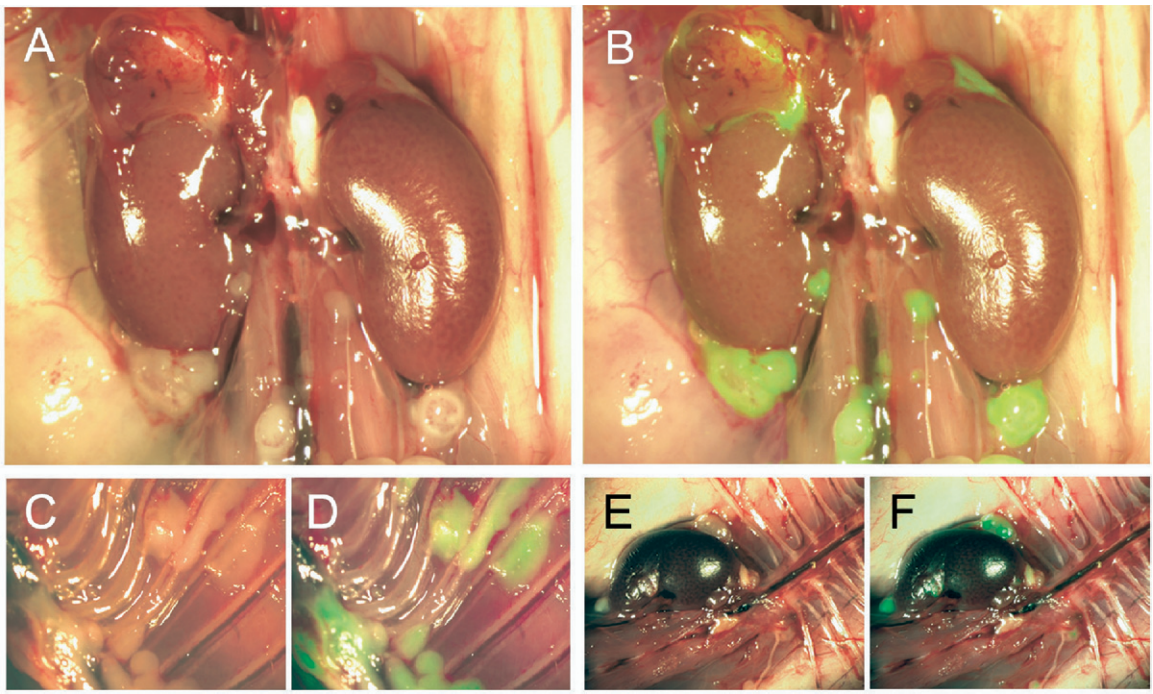

Figure 6. Virally guided fluorescent detection of lymph node metastases. A pleural mesothelioma model was developed by injecting mesothelioma cells into the pleural cavities of mice. Four to 8 weeks after tumor implantation, mice were treated with 2 doses of NV1066 injected intrapleurally. After treatment, mice were killed, and retroperitoneal and mediastinal areas were examined under bright-field (A, C, and E) and fluorescent (B, D and F) modes. Green fluorescent protein (*GFP*) expression facilitated easy identification of metastatic lymph nodes (LNs) that were not obvious on bright-field examination (used with permission: copyright © 2006 by The Federation of American Societies for Experimental Biology. Adusumilli et al. 2006 Fig 5, *A* and *B*).

ral LNs.[E25] Furthermore, diaphragmatic mesothelioma might also involve retroperitoneal LNs and the lymphatics of the gastrohepatic ligament and celiac axis.[E25] Extrapleural nodal metastases from MPM are related to poor survival.[E2,E5-E7,E26,E27] Patterns of tumor recurrence after trimodality therapy for MPM reveal that 26% recur in the peritoneum, 17% in the contralateral pleura, and 8% at distant site.[E6] Therefore it is important to accurately identify the LN metastases in MPM to select the resectable and curable patients for surgical intervention.[E2,E3,E5,E7,E8]

We introduce a novel method of real-time fluorescent lymphatic mapping that uses cancer cell–specific viral production of GFP to detect tumor cells in LNs. By incorporating a strain of HSV that contains the marker gene for GFP, we hope to expand the role of viral gene therapy from one that is purely therapeutic to one that is also diagnostic and can be used in surgical applications.[E23,E24,E28] We have shown that NV1066 localizes metastatic LNs after administration into the primary tumor, where it infects cancer cells. Infection results in expression of GFP at metastatic sites that can be visualized by using novel in vivo fluorescent imaging modalities, such as thoracoscopy and mediastinoscopy.[E23,E24] The real-time intraoperative detection of LN metastases distinguishes this technique from other LN-localizing methods. Theoretic advantages of such a technique include (1) improved accuracy and thorough sampling of the metastatic LNs that are not obvious on cursory examination and (2) reduced human error.

To date, we have shown that NV1066 infects and expresses GFP in more than 18 thoracic malignancy–derived cancer cell lines.[E11,E19,E24,E28,E29] GFP can be detected as early as 2 to 4 hours after viral infection. NV1066 carries "enhanced" GFP, which produces a stronger fluorescent signal and matures faster than conventional GFP, reducing the lag time between synthesis and detection.[E23] Furthermore, amplification of the administered viral dose enables treatment with low viral titers.[E11,E23,E24] The difference in the peaks of cellular autofluorescence and NV1066-induced enhanced GFP reduces the risk that autofluorescence will provide false-positive results. Detection of microscopic foci of cancer by using GFP is quite sensitive; our in vitro data suggest that as few as 10 clustered cells might be identified, a limit of detection significantly lower than that of other imaging techniques (ie, CT, magnetic resonance imaging, and PET scans cannot

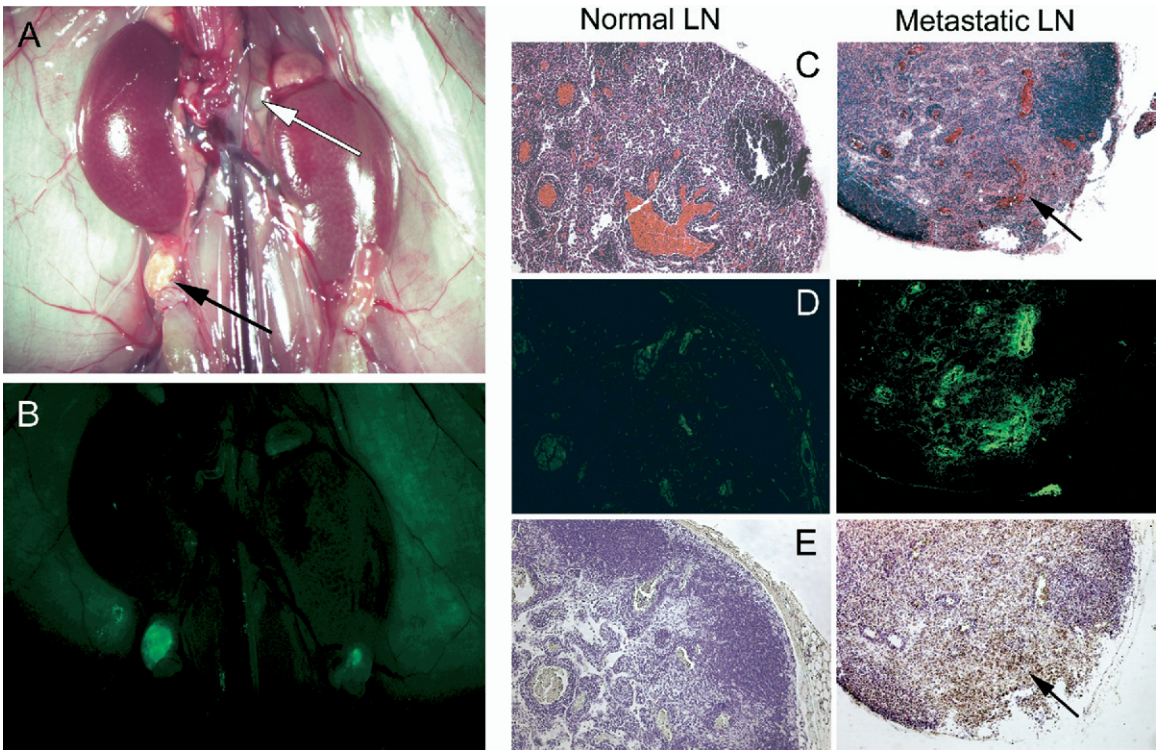

Figure 7. Viral specificity to metastatic lymph nodes *(LN)* was confirmed by means of immunohistochemistry. In representative mice with pleural mesothelioma, after NV1066 treatment (A), green fluorescent protein (*GFP*) expression facilitated identification of metastatic LNs (B). Both normal and metastatic LNs were serially sectioned, and identical sections were stained with hematoxylin and eosin (C), observed under fluorescent microscopy (D), and stained with herpes simplex virus (*HSV-1*) polyclonal antibody (E). The presence of tumor in the metastatic LN was identified by an *arrow* (C, metastatic LN), which correlated with GFP expression (D, metastatic LN). Viral specificity to the metastatic area was confirmed by means of immunohistochemistry (E, metastatic LN). The absence of GFP expression and HSV-1 antibody staining in normal LNs further confirmed viral specificity to the tumor in metastatic LNs.

GTS

detect tumor foci smaller than 3-4 mm in size or approximately 1×10^7 cells).[E24] Studies have indicated that fluorescent intensity ratios of 3 or greater are sufficient to distinguish between induced fluorescence in tumors and background autofluorescence in normal tissues.[E24] As demonstrated in this study, the fluorescent intensity ratios are several logs higher between infected cancer tissue and normal tissue and thereby facilitate easy identification of even microscopic deposits by means of fluorescent thoracoscopy.

The diagnostic potential of HSV to detect microscopic cancer is not limited by the route of administration. Biodistribution studies from our laboratory using radiolabeled virus have demonstrated that tumor-targeted delivery of NV1066 is not affected by the route of delivery (data not published). Where feasible, HSV can be delivered into body cavities through a simple intrapleural or intraperitoneal injection the day before. Although other LN-localizing methods are purely diagnostic, the use of oncolytic herpes viruses might confer an additional therapeutic advantage. Extensive work in our laboratory and others has demonstrated that oncolytic HSV strains are highly effective in the treatment of a wide variety of experimental models of cancer, including lung cancer,[E19] esophageal cancer,[E29] gastric cancer,[E10,E22] and MPM.[E9,E11] Systemic or intrapleural administration of HSV resulted in reduced tumor burden and increased survival. Potentially, HSV used to detect disease might also be able to reduce both primary site recurrence and regional nodal metastases.[E18]

This proof-of-concept study also demonstrates that herpes-guided GFP detection of lymphatic metastases can be a highly sensitive and specific technique, comparing favorably with standard methods. All sections expressing GFP were confirmed to be harboring tumor by means of histology and immunohistochemistry. HSV was localized to the GFP-expressing tumor, as evident by using immunohistochemistry. Furthermore, GFP expression can facilitate ac-

curate and quick identification of microscopic foci of tumor in histologic sections without any additional need for staining, thereby enhancing the detection of tumor in frozen sections.

One limitation of this study is the lack of data to further define the predicted value of this technique. Rapid and fully automated quantitative RT-PCR assays are being developed to detect metastatic tumor in LNs with equal operating characteristics compared with conventional histology.[E30] Our laboratory has demonstrated that in detecting LN metastases from breast cancer, HSV-guided, GFP-mediated lymphatic mapping demonstrated favorable operating characteristics (sensitivity, 80%; specificity, 96%) when compared with other molecular methods (quantitative RT-PCR) of detection.[E31] Similar studies attempting to further define the sensitivity and specificity of GFP-guided LN detection in thoracic malignancies have been constrained by the practical limitations of quantifying pleural malignancy by means of molecular methods and the relative inconsistency of metastatic LN frequency.

Oncolytic herpes viruses are highly specific for infection of cancer cells, sparing normal cells.[E15,E18,E23,E24,E28,E29] The mechanisms of cancer cell–selective infection and replication of oncolytic viruses are discussed in detail elsewhere.[E15-E17] Investigations with NV1066 and other oncolytic HSV strains have shown no observable toxicity in rodent models.[E18,E23,E24,E29] Furthermore, immunohistochemical and PCR analyses consistently demonstrated the absence of viral particles in noncancerous tissues.[E11,E23] The safety of HSV has been tested in preclinical toxicology studies in *Aotus trivigatus* monkeys, which are exquisitely sensitive to wild-type herpes viral infections.[E32,E33] These monkeys demonstrated no toxicity when administered attenuated virus.[E32,E33] Additionally, the favorable safety profile of parental oncolytic HSV strains has been established in phase I and II human clinical trials.[E15,E34-E36] Preliminary results of a multicenter, phase I/II, open-label study of NV1020 administered by means of hepatic artery infusion has shown an excellent safety profile in patients with colorectal adenocarcinoma to the liver, and the efficacy is currently being evaluated.[E37] Clinical trials with other oncolytic viruses pointed out hurdles, such as limitation of systemic distribution, intratumoral spread, and immune responses. To overcome these hurdles, we have used a multimodal cancer treatment approach combining NV1066 with standard radiotherapy, chemotherapy, and gene therapy to enhance antitumor efficacy without overlapping toxicities or resistance. Diagnostic gene therapy with an oncolytic virus, as described in this article, is an entirely new paradigm and needs to be assessed in future clinical trails.

This technology holds promise for improving patient care for MPM and a number of other thoracic malignancies. Pilot studies conducted in our laboratory have shown that similar results of fluorescent lymphatic detection are possible in lung and esophageal cancer. The accurate assessment of LN involvement in an intraoperative setting might affect the therapeutic decision in the surgical management of thoracic malignancies.

We thank Medigene, Inc, for constructing and providing us with the NV1066 virus. We thank Liza Marsh of the Department of Surgery at Memorial Sloan-Kettering Cancer Center for her editorial assistance. Special thanks to Kan Matsumoto from Olympus America, Inc, for design and construction of the fluorescent thoracoscopic system.

Discussion

Dr Mark J. Krasna *(Baltimore, Md)*. I have a couple of technical questions, if you can answer. The article was very well written. One of the things that was not clear to me, though, was how large these animals were. It said 4 to 8 weeks. I am very impressed at your thoracoscopic and laparoscopic skills. Can you tell us how many kilos or grams these animals weighed?

Dr Adusumilli. These mice typically weigh 30 to 50 g. Most of these pictures were taken after the mice were killed. In addition, we removed the internal organs after killing the animal, so that the chest and abdominal cavity were well exposed. In intact animals we injected air or carbon dioxide into the abdominal cavity to improve visualization.

Dr Krasna. This was still done with a 5-mm optic scope?

Dr Adusumilli. Yes.

Dr Marc Ruel *(Ottawa, Canada)*. Can you please comment about the future applicability of this method to human subjects, first with respect to the biosafety of using such an approach and then with respect to the future clinical sensitivity that you expect with this approach, because obviously the model that you have in the mouse has a high pretest probability for LN positivity, but what about in human subjects with the hardships of, for example, fluorescent thoracoscopy? Thank you.

Dr Adusumilli. I would like to first answer the question about sensitivity. Viral infection and fluorescence are selective to cancer cells. In this pilot study we used the immunohistochemical methods to confirm virus selectivity to cancer cells. We do know that right now the standard is RT-PCR, in which methods are being developed to detect cancer cell tumor markers within 30 minutes. We conducted experiments in a mouse breast cancer model and compared the sensitivity with that of RT-PCR. We developed breast cancer in the mammary fat pad, treated the primary tumor with NV1066, and then harvested the axillary and thoracic LNs. We tested both fluorescent and nonfluorescent LNs for tumor marker using RT-PCR. As you can see in this slide, the initial pilot studies have shown a sensitivity of about 80% and a specificity of about 96%.

In regard to the practical limitations of fluorescent thoracoscopy, we do know that there might be a practical problem of detecting a micrometastasis hidden deep in an LN. Having said that, the GFP excitation wavelength is very specific. In the future, fluorescent endoscopy can be combined with computer detection models to accurately pinpoint GFP-expressing cancerous areas, just like what is being done with FDG probes now.

In addition, the actual property of this virus is oncolytic. Even if you miss the green fluorescence and micrometastases, the virus replicates and then kills the infected cancer cells. In vitro all 11 cell lines were killed at a higher MOI of 1. However, as you pointed out, in the clinical setting we might not be able to administer an MOI of 1. Therefore we tested with an MOI of 0.01 (ie, 1 viral plaque-forming unit per 100 cancer cells). As you can see in this representation, although the sensitivity differs, more than 50% of all the cancer cells were lysed by day 7. In regard to human studies, phase 1 is completed, and a multicenter phase 2 trial is in progress testing oncolytic HSV therapy for colorectal metastases in the liver. We are optimistic that in addition to being a therapeutic tool, oncolytic HSV can be a surgeon's tool that can be used for diagnostic purposes.

Dr Vivek Rao *(Toronto, Canada)*. Just to expand on the theme of clinical applicability, correct me if I am wrong, but does this technique not require a direct inoculation of the primary tumor? Therefore if you take yourself to the operating room and you are resecting, let us say, a primary lung tumor, you are not going to be able to identify at the time of your thoracotomy where your metastases or potential metastases are located. Is this a technique to come back later? And if it is a technique to come back later and do surveillance thoracoscopy, if you remove the primary tumor, how do you then inoculate the patient?

Dr Adusumilli. Thank you. We intend to use the virus before resection of the primary tumor. To ensure such applicability, we tested 2 methods: locally by means of primary inoculation directly into the tumor and systemically as injections through the tail vein of the mice and rat. Irrespective of the method, the virus is able to infect and fluoresce specifically in cancer cells. We also realized the potential problem of immunity. Therefore we tested both in immunocompetent and immunodeficient models with systemic and local injections. The local injections are much better to ensure high infectivity. Systemic injections were still effective, although the infectivity and peak of viral replication was delayed. However, the viral specificity is still maintained. In immunocompetent animal models, hamster cheek pouch and SENCAR pouch, where spontaneous cancers arise after local application of the chemical carcinogen, again, as you can see here, viral infection was very specific to the cancer area. Therefore both in immunocompetent and in immunodeficient models, direct application is better than systemic application, and with both methods, one can still get the results. In the thoracic cavity, with bronchoscopic injections, CT-guided injections, or thoracoscopic direct injections, inoculation of the primary tumor can be achieved.

Dr Michael Chris Lekas *(Toronto, Canada)*. I have several quick questions. Did you look at the possibility that cells, once they were transfected with HSV, transformed into something even more aggressive and potentially malignant? I know you had impressive kill ratios, but they are obviously not 100%, and in some it was only 50%.

Dr Adusumilli. In the experimental setting, in vitro, it is difficult to continue the experiment beyond 7 to 9 days, and therefore it appears that only 50% of the cells are lysed in certain cell lines. In reality, all the infected cancer cells were lysed. The cytotoxicity and sensitivity depend on the individual cell type, receptors on the cancer cell, and replicative mechanisms in the cancer cell. At the end of the day, as long as the viral replication is continued, the cancer cells were lysed. This is going to be the key in clinical applications. Initially we tested high doses, but we wanted to avoid any possible side effects. Therefore the key is going to be using low doses and ensuring continuation of viral replication localized to the tumor. This is achieved by combining oncolytic viral therapy with radiation therapy or chemotherapy. Both these therapies enhance stress genes in cancer cells, which the virus uses for its advantage to enhance replication. Therefore we believe that by using localized focused radiation or, in the case of colorectal metastases, the phase I model, by infusing chemotherapy through the pump in the hepatic artery (ie, localized chemotherapy infusions), we can keep the viral replication enhanced in the tumor. Recently, we presented our data at the Federation of American Societies of Experimental Biology indicating that by combining with hyperthermia, oncolytic viral replication is enhanced. Therefore by combining the therapeutic modalities, by localizing the virus, and by continuing the viral replication, even the cancer cells that are resistant to an individual therapy can be lysed.

References

E1. Antman KH. Natural history and epidemiology of malignant mesothelioma. *Chest.* 1993;103(suppl):373S-376S.

E2. Sugarbaker DJ, Flores RM, Jaklitsch MT, Richards WG, Strauss GM, Corson JM, et al. Resection margins, extrapleural nodal status, and cell type determine postoperative long-term survival in trimodality therapy of malignant pleural mesothelioma: results in 183 patients. *J Thorac Cardiovasc Surg.* 1999;117:54-63.

E3. Pilling JE, Stewart DJ, Martin-Ucar AE, Muller S, O'Byrne KJ, Waller DA. The case for routine cervical mediastinoscopy prior to radical surgery for malignant pleural mesothelioma. *Eur J Cardiothorac Surg.* 2004;25:497-501.

E4. Heelan RT, Rusch VW, Begg CB, Panicek DM, Caravelli JF, Eisen C. Staging of malignant pleural mesothelioma: comparison of CT and MR imaging. *AJR Am J Roentgenol.* 1999;172:1039-47.

E5. Flores RM, Akhurst T, Gonen M, Larson SM, Rusch VW. Positron emission tomography defines metastatic disease but not locoregional disease in patients with malignant pleural mesothelioma. *J Thorac Cardiovasc Surg.* 2003;126:11-6.

E6. Janne PA, Baldini EH. Patterns of failure following surgical resection for malignant pleural mesothelioma. *Thorac Surg Clin.* 2004;14:567-73.

E7. Alvarez JM, Ha T, Musk W, Robins P, Price R, Byrne MJ. Importance of mediastinoscopy, bilateral thoracoscopy, and laparoscopy in correct staging of malignant mesothelioma before extrapleural pneumonectomy. *J Thorac Cardiovasc Surg.* 2005;130:905-6.

E8. Rice DC, Erasmus JJ, Stevens CW, Vaporciyan AA, Wu JS, Tsao AS, et al. Extended surgical staging for potentially resectable malignant pleural mesothelioma. *Ann Thorac Surg.* 2005;80:1988-92.

E9. Adusumilli PS, Chan MK, Chun YS, Hezel M, Chou TC, Rusch VW, et al. Cisplatin-induced GADD34 upregulation potentiates oncolytic viral therapy in the treatment of malignant pleural mesothelioma. *Cancer Biol Ther.* 2006;5:48-53.

E10. Adusumilli PS, Eisenberg DP, Chun YS, Ryu KW, Ben-Porat L, Hendershott KJ, et al. Virally directed fluorescent imaging improves diagnostic sensitivity in the detection of minimal residual disease after potentially curative cytoreductive surgery. *J Gastrointest Surg.* 2005;9:1138-47.

E11. Adusumilli PS, Stiles BM, Chan MK, Mullerad M, Eisenberg DP, Ben-Porat L, et al. Imaging and therapy of malignant pleural mesothelioma using replication-competent herpes simplex viruses. *J Gene Med.* 2006;8:603-15.

E12. Kucharczuk JC, Randazzo B, Chang MY, Amin KM, Elshami AA, Sterman DH, et al. Use of a "replication-restricted" herpes virus to treat experimental human malignant mesothelioma. *Cancer Res.* 1997;57:466-71.

E13. van der Most RG, Robinson BW, Nelson DJ. Gene therapy for malignant mesothelioma: beyond the infant years. *Cancer Gene Ther.* 2006 [epub ahead of print].

E14. Sterman DH, Recio A, Vachani A, Sun J, Cheung L, DeLong P, et al. Long-term follow-up of patients with malignant pleural mesothelioma receiving high-dose adenovirus herpes simplex thymidine kinase/ganciclovir suicide gene therapy. *Clin Cancer Res.* 2005;11:7444-53.

E15. Everts B, van der Poel HG. Replication-selective oncolytic viruses in the treatment of cancer. *Cancer Gene Ther.* 2005;12:141-61.

E16. Lou E. Oncolytic herpes viruses as a potential mechanism for cancer therapy. *Acta Oncol.* 2003;42:660-71.

E17. Shen Y, Nemunaitis J. Herpes simplex virus 1 (HSV-1) for cancer treatment. *Cancer Gene Ther.* 2006. [epub ahead of print].

E18. Wong RJ, Joe JK, Kim SH, Shah JP, Horsburgh B, Fong Y. Oncolytic herpesvirus effectively treats murine squamous cell carcinoma and spreads by natural lymphatics to treat sites of lymphatic metastases. *Hum Gene Ther.* 2002;13:1213-23.

E19. Adusumilli PS, Stiles BM, Chan MK, Chou TC, Wong RJ, Rusch VW, et al. Radiation therapy potentiates effective oncolytic viral therapy in the treatment of lung cancer. *Ann Thorac Surg.* 2005;80: 409-16.

E20. Sterman DH, Treat J, Litzky LA, Amin KM, Coonrod L, Molnar-Kimber K, et al. Adenovirus-mediated herpes simplex virus thymidine kinase/ganciclovir gene therapy in patients with localized malignancy: results of a phase I clinical trial in malignant mesothelioma. *Hum Gene Ther.* 1998;9:1083-92.

E21. Ino Y, Saeki Y, Fukuhara H, Todo T. Triple combination of oncolytic herpes simplex virus-1 vectors armed with interleukin-12, interleukin-18, or soluble B7-1 results in enhanced antitumor efficacy. *Clin Cancer Res.* 2006;12:643-52.

E22. Stanziale SF, Stiles BM, Bhargava A, Kerns SA, Kalakonda N, Fong Y. Oncolytic herpes simplex virus-1 mutant expressing green fluorescent protein can detect and treat peritoneal cancer. *Hum Gene Ther.* 2004;15:609-18.

E23. Adusumilli PS, Stiles BM, Chan MK, Eisenberg DP, Yu Z, Stanziale SF, et al. Real-time diagnostic imaging of tumors and metastases by use of a replication-competent herpes vector to facilitate minimally-invasive oncological surgery. *FASEB J.* 2006;20:726-8.

E24. Stiles B, Adusumilli P, Bhargava A, Stanziale S, Kim T, Chan M, et al. Minimally-invasive localization of oncolytic herpes simplex viral therapy of micrometastatic pleural cancer. *Cancer Gene Ther.* 2006; 13:53-64.

E25. Sharma A, Fidias P, Hayman LA, Loomis SL, Taber KH, Aquino SL. Patterns of lymphadenopathy in thoracic malignancies. *Radiographics.* 2004;24:419-34.

E26. Rusch VW, Venkatraman ES. Important prognostic factors in patients with malignant pleural mesothelioma, managed surgically. *Ann Thorac Surg.* 1999;68:1799-804.

E27. Baldini EH, Recht A, Strauss GM, DeCamp MM Jr, Swanson SJ, Liptay MJ, et al. Patterns of failure after trimodality therapy for malignant pleural mesothelioma. *Ann Thorac Surg.* 1997;63:334-8.

E28. Adusumilli PS, Eisenberg DP, Stiles BM, Hendershott KJ, Stanziale SF, Chan MK, et al. Virally-directed fluorescent imaging (VFI) can facilitate endoscopic staging. *Surg Endosc.* 2006;20:628-35.

E29. Stiles BM, Bhargava A, Adusumilli PS, Stanziale SF, Kim TH, Rusch VW, et al. The replication-competent oncolytic herpes simplex mutant virus NV1066 is effective in the treatment of esophageal cancer. *Surgery.* 2003;134:357-64.

E30. Hughes SJ, Xi L, Raja S, Gooding W, Cole DJ, Gillanders WE, et al. A rapid, fully automated, molecular-based assay accurately analyzes sentinel lymph nodes for the presence of metastatic breast cancer. *Ann Surg.* 2006;243:389-98.

E31. Eisenberg DP, Adusumilli PS, Hendershott KJ, Chung S, Yu Z, Chan MK, et al. Real-time intraoperative detection of breast cancer axillary lymph node metastases using a green fluorescent protein-expressing herpes virus. *Ann Surg.* 2006;243:824-32.

E32. Meignier B, Martin B, Whitley R, Roizman B. In vivo behavior of genetically engineered herpes simplex viruses R7017 and R7020. 11. Studies in immunocompetent and immunosuppressed owl monkeys *(Aotus trivigatus)*. *J Infect Dis.* 1999;162:313-21.

E33. Todo T, Feigenbaum F, Rabkin SD, Lakeman F, Newsome JT, Johnson PA, et al. Viral shedding and biodistribution of G207, a multimutated, conditionally replicating herpes simplex virus type 1, after intracerebral inoculation in aotus. *Mol Ther.* 2000;2:588-95.

E34. Rampling R, Cruickshank G, Papanastassiou V, Nicoll J, Hadley D, Brennan D, et al. Toxicity evaluation of replication-competent herpes simplex virus (ICP 34.5 null mutant 1716) in patients with recurrent malignant glioma. *Gene Ther.* 2000;7:859-66.

E35. Markert JM, Medlock MD, Rabkin SD, Gillespie GY, Todo T, Hunter WD, et al. Conditionally replicating herpes simplex virus mutant, G207 for the treatment of malignant glioma: results of a phase I trial. *Gene Ther.* 2000;7:867-74.

E36. Latchman DS. Herpes simplex virus-based vectors for the treatment of cancer and neurodegenerative disease. *Curr Opin Mol Ther.* 2005;7:415-8.

E37. Chari R, Gevargheese S, Nemunaitis J, Fong Y, Tanabe K, Galanis E, et al. A phase I/II, open-label study (with a sequential dose escalation stage followed by an expansion of a selected dose cohort), to evaluate the safety and anti-tumor effects of an oncolytic Herpes simplex virus, NV1020, administered repeatedly via hepatic artery infusion prior to second-line chemotherapy, in patients with colorectal adenocarcinoma metastatic to the liver. Abstract presented at Digestive Diseases Week, May 20-25, 2006, Los Angeles, California.